Electronic Supplementary Information

for

Polyaniline-decorated porous carbons with engineered meso/macro-channels for High performance capacitive deionization

Bofeng Li[a], Qi Cao[a], Ya Liu[a,b], Yukuo Sun[a], Xinlong Ma[a], Xiaoguang Duan[b], Chunmao Chen[a], and Yuxian Wang[a,*]

[a] State Key Laboratory of Heavy Oil Processing, State Key Laboratory of Petroleum Pollution Control, China University of Petroleum-Beijing, Beijing 102249, China.

[b] School of Chemical Engineering and Advanced Materials, The University of Adelaide, Adelaide, SA 5005, Australia

*Corresponding Author

E-mail address: yuxian.wang@cup.edu.cn

Text S1. Synthesis of PACs and PAC/mPANI

Porous activated carbon (PAC) was prepared as follow. First, 30 g KOH and 10 g asphalt powder were transferred in the mechanic blender and ground them up until they were well mixed. Then the mixture was placed in the die of the tableting press and 10 MPa pressure was applied. After that, the pressed sample was sintered under Ar atmosphere from room temperature to 800 °C for 1 h and allowed to naturally cool down to room temperature. The heating ramp was set as 10 °C min^{-1}. After the heat treatment, the sample was washed by HCl solution (1 M) and deionized water (V_{HCl}:V_{DI} = 1:3) for 3 times to remove any impurities. The resultant black solid material was dried in vacuum at 60 °C for 12 h and denoted as PAC-10. Similarly, PAC-0, PAC-5, PAC-8, PAC-12, and PAC-15 were synthesized with no pressure, 5 MPa, 8 MPa, 12 MPa, and 15 MPa pressure was applied, respectively.

PAC/20PANI was synthesized via oxidative polymerization with PAC-10 as the precursor. First, 200 μL of aniline (which was 20 wt.% of PAC-10) was dispersed into a mixture solution containing 20 mL 1 M HCl solution and 2 mL ethanol. The mixture was stirred in an ice bath for 10 min. After that, 1 g of PAC-10 was dispersed into the above solution under stirring for 30 min to form the solution A. After that, 500 mg of ammonium persulfate (APS) was dissolved in 2.5 mL 1 M HCl to form the solution B. Subsequently, solution B was added to solution A under vigorous stirring. This dispersion solution was kept stirring in an ice bath for 12 h. Then, the product was collected by vacuum filtration and washed thoroughly with deionized water and ethanol until the filtrate changed from emerald green to colorless. This resultant filter cake was then dried at 60 ºC for 24 h to obtain PAC/20PANI. PAC/10PANI and PAC/30PANI were also synthesized by the similar procedures except 10 wt.% and 30 wt.% aniline was added. To compared PAC-0/20PANI was synthesized with PAC-0 as the precursor.

Text S2. Detailed description of the characterization methods

Morphologies of the samples were observed on a Quanta 200F SEM at an accelerating voltage of 5 kV. Transmission electron microscopy (TEM) images were obtained from JEOL 2100F (UHR). The TEM instrument was employed to provide in-depth structural information. Moreover, N_2 sorption isotherms were acquired on JW-BK222 to measure the Brunauer–Emmett–Teller (BET) specific surface areas (SSA) and Barrett-Joyner-Halenda (BJH) pore size distribution. Prior to the testing, the samples were degassed at 100 ℃ overnight under vacuum condition. Surface composition of the carbon materials were characterized by X-ray photoelectron microscopy (XPS, 2PHI Quantera scanning X-ray microprobe) under ultra-high vacuum (UHV) condition with Al–Kα X-ray irradiation. FT-IR was performed in the range 400–4000 cm^{-1} to characterize the changes in organic functional groups and carbon materials is complexed with KBr (material: KBr=1: 200). Raman spectra of the samples were recorded by a Renishaw RM2000 Raman spectrometer with the wavelength of 532 nm. Dynamic contact angle measurements of as-obtained materials in water systems were performed on the optical contact angle & interface tension meter (SL200KS, USA). Electrical conductivity of solid powder materials was measured by multifunctional automatic resistivity meter (GM-II, Weida).

Text S3. Preparation of electrode materials

The electrode slurry was prepared by mixing 80 wt.% as-synthesized materials, 10 wt.% conductive carbon black, 10 wt.% poly-vinylidine fluoride (PVDF), and a trace amount of N-methylpyrrolidone (NMP). The obtained slurry was uniformly painted on the current collector of and dried for 12 h at 100 °C in a vacuum oven. The electrode plates for three-electrode test, two-electrode test and capacitive desalination test were 1×1 cm^2 carbon cloth, d=13 mm carbon cloth and 5×5 cm^2 graphite paper, respectively. In a three-electrode system, 0.5 M NaCl solution was used as the electrolyte, CV

measurements were performed at scan rate of 5 mv s^{-1} at a voltage window range of −0.2 to 0.8 V. GCD tests were conducted at a current density 1 A g^{-1} with a potential window range of −0.2 to 0.8 V. The electrochemical impedance spectroscopy (EIS) was tested in the frequency range of 0.01 Hz to 100 KHz of 10 mV amplitude. In a two-electrode system, 1 M Na_2SO_4 solution and glass microfiber (Whatman, GF/D1823-047) were used as the electrolyte and separator, respectively. The mass loading of the as-synthesized materials for each electrode was about 2 mg. GCD tests were conducted at a current density 1 A g^{-1} with a potential window range of 0 to 1.2 V.

Table S1. The SSA and pore size distribution of PAC-n and PAC/mPANI.

Sample	SSA ($m^2\ g^{-1}$)	V_{total} ($cm^3\ g^{-1}$)	V_{mic} ($cm^3\ g^{-1}$)	$V_{mac/mes}$ ($cm^3\ g^{-1}$)
PAC-0	2983	1.63	1.30	0.33
PAC-5	2991	1.64	1.14	0.51
PAC-8	2997	1.67	1.15	0.51
PAC-10	3002	1.68	1.14	0.54
PAC-12	2981	1.63	1.11	0.53
PAC-15	2979	1.60	1.08	0.52
PAC/30PANI	1816	1.03	0.66	0.37
PAC/20PANI	2176	1.26	0.85	0.41
PAC/10PANI	2498	1.45	1.02	0.430
PAC-0/20PANI	2146	1.21	0.83	0.38

Table S2. XPS full survey and high-resolution XPS surveys of C 1s region for the as-synthesized PAC-10 and PAC/mPANI.

Material	**Full Survey**			**High resolution C1s survey**					
	C (at%)	N (at%)	O (at%)	sp^2 C (at%)	sp^3 C (at%)	C–OH (at%)	–C=O (at%)	O–C=O (at%)	π–π shake up (at%)
PAC-10	94.6	0	5.4	47.9	24.3	11.4	6.3	6.5	3.6
PAC/10PANI	91.9	1.5	6.1	48.7	22.5	11.6	6.6	6.7	3.9
PAC/20PANI	91.4	2.1	6.5	49.1	20.3	11.9	7.1	6.8	4.8
PAC/30PANI	90.0	3.4	6.6	49.7	18.7	12.3	7.3	6.9	5.1

Table S3. High-resolution XPS surveys of N 1s and O 1s region for the as-synthesized PAC-10 and PAC/mPANI.

Material	High resolution N1s survey			High resolution O1s survey		
	–N= (at%)	–NH– (at%)	–N+ (at%)	–C=O (at%)	–C–O/–NO_x (at%)	Chemisorbed water (at%)
PAC-10	-	-	-	53.7	33.8	12.5
PAC/10PANI	39.3	32.0	28.7	59.0	30.8	10.2
PAC/20PANI	37.3	33.2	29.5	58.7	29.6	11.7
PAC/30PANI	32.7	34.8	32.4	54.4	34.5	11.1

Table S4. Potential of zero charge (E_{pzc}), short circuit potential (E_0), and their potential difference (ΔE) of PACs and PAC/mPANI.

Sample	E_{pzc} (V)	E_0	ΔE
PAC-0	0.1501	0.0938	0.0563
PAC-5	0.1539	0.1126	0.0413
PAC-10	0.1478	0.1146	0.0332
PAC-15	0.1473	0.1357	0.0116
PAC/10PANI	0.1355	0.1241	0.0114
PAC/20PANI	0.1758	0.1729	0.0029
PAC/30PANI	0.1347	0.1241	0.0106
PAC-0/20PANI	0.1750	0.1620	0.013

Table S5. Comparison of salt adsorption capacity and stability with PAC/20PANI and previous literatures.

Material	Voltage (V)	Initial salt concentration (mg L^{-1})	SAC (mg g^{-1})	Two electrodes Cycle number	Retention rate	Specific capacity (F g^{-1})	Ref.
CPC	1.2	1500–1700	18.9	300	92%	168.2	[1]
HMYSC	1.4	500	16.1	-	-	204	[2]
PaniT-AC	1.4	500	30.5	-	-	237	[3]
N-PC	1.2	500	22.4	-	-	229	[4]
NPC	1.2	500	21.4	100	97%	163	[5]
3DGA-OP	1.2	500	14.4	-	-	160	[6]
hierarchically porous non-carbon	1.2	500	23.6	-	-	171	[7]
PAC/20PANI	1.2	500	35.3	20000	97.06%	247	This work

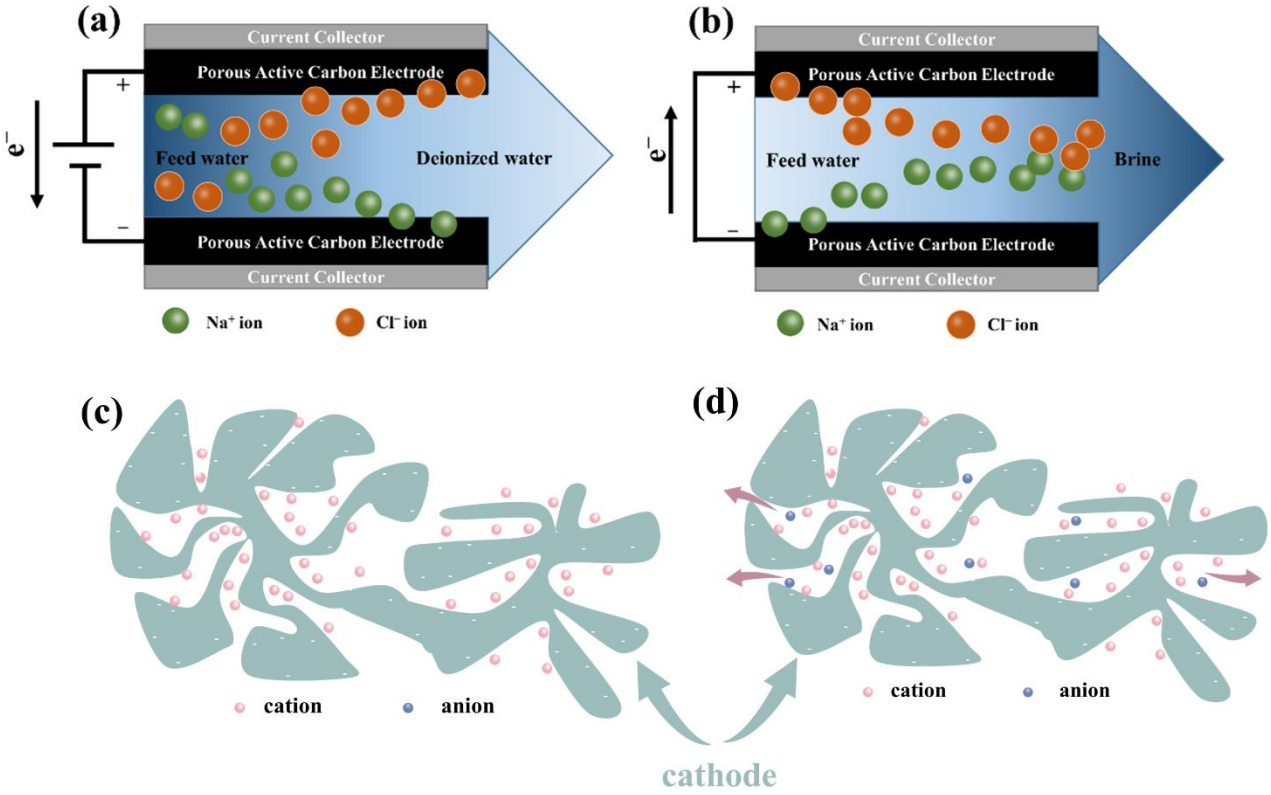

Figure S1. (a) Schematic illustration of a typical CDI process; (b) The regeneration process proceeds by short circuiting Counter-ion adsorption on CDI electrode; (c) Schematic illustration of counter ion adsorption on the negatively charge electrode; (d) Schematic illustration of co-ion desorption or ion swapping (ion exchange) on the negatively charge electrode.

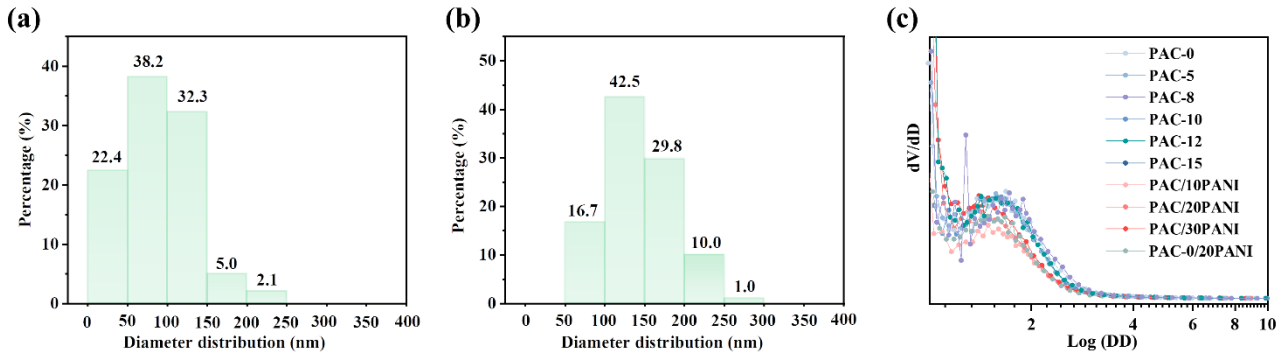

Figure S2. Statistics of pore size distribution of PACs prepared tablet pressure based on SEM images: 0 MPa (a); 10 MPa (b); BJH desorption pore volume distribution of Log (DD/nm)-dV/dD for PACs and PAC/PANIs (c).

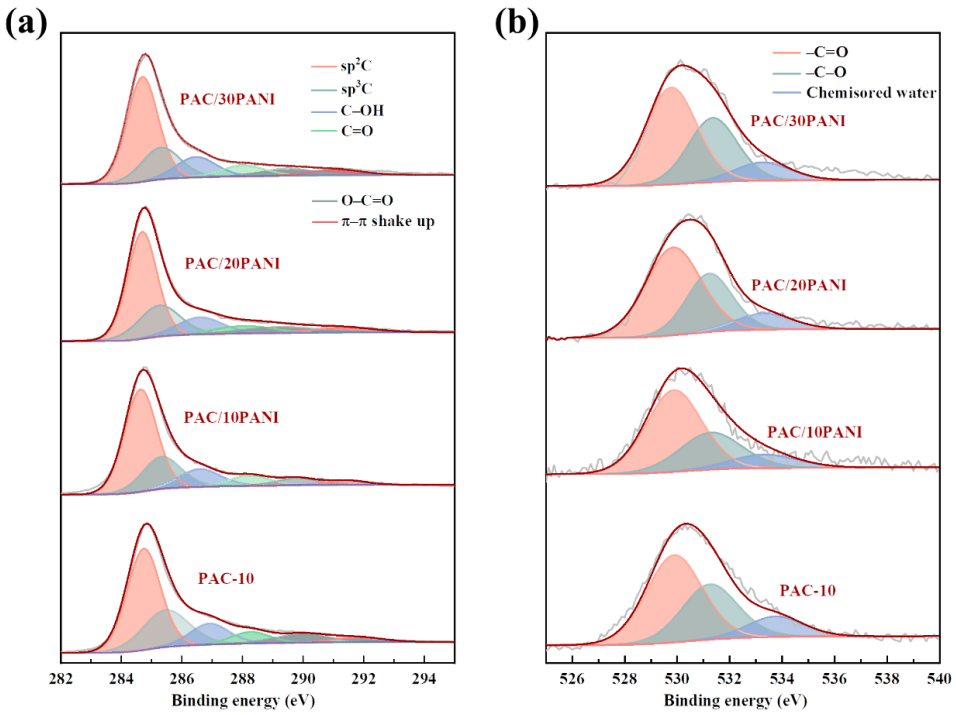

Figure S3. High-resolution XPS spectra of PAC-10 and PAC/mPANI: C 1s (a); O 1s (b).

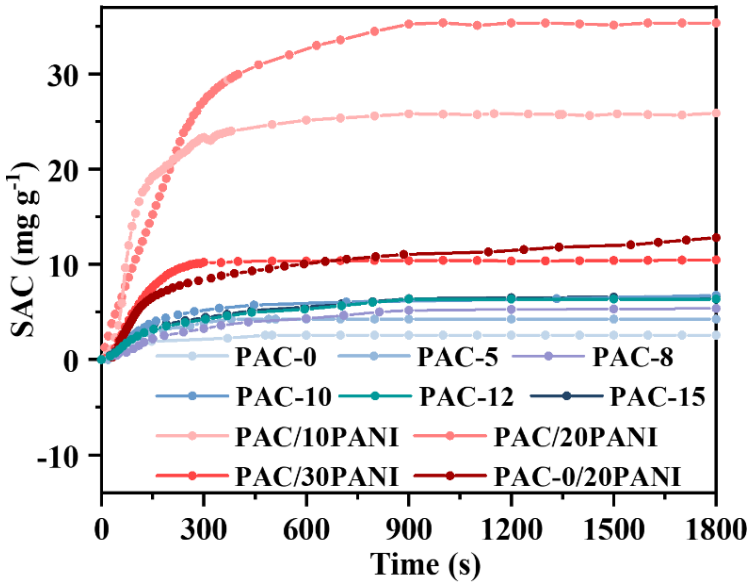

Figure S4. The SAC of PACs and PAC/PANIs.

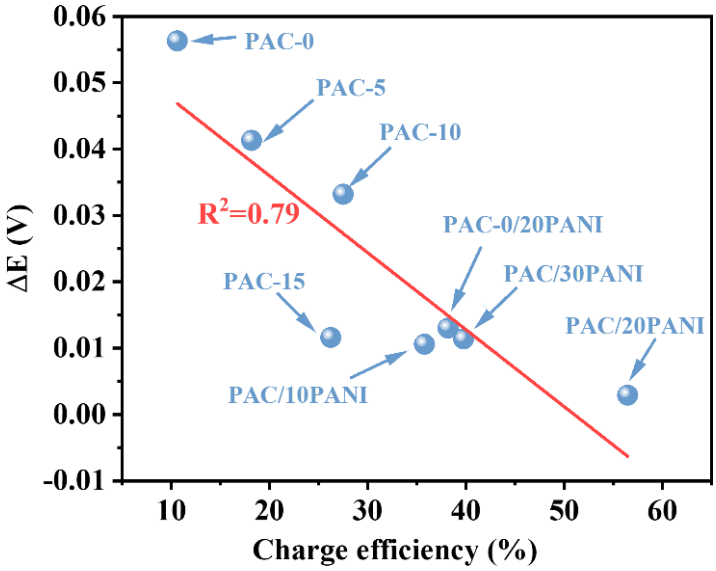

Figure S5. Correlation between ΔE and SAC for PACs and PAC/PANIs.

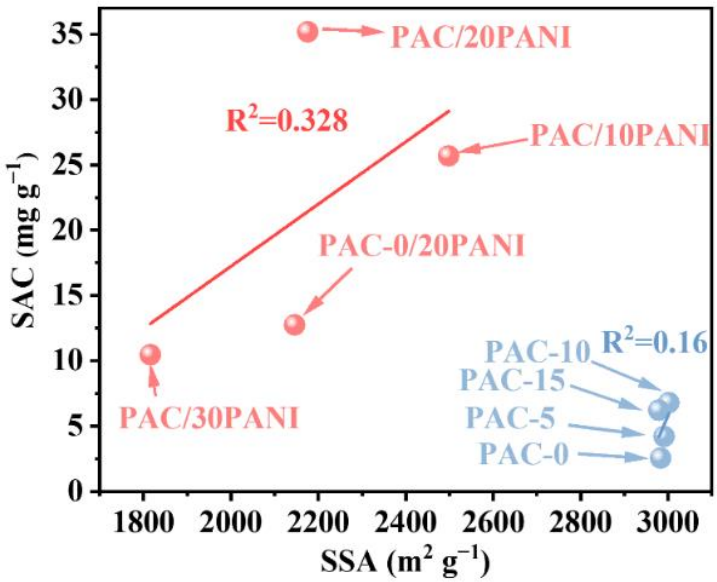

Figure S6. Correlation between SSA and the SAC for PACs and PAC/mPANI.

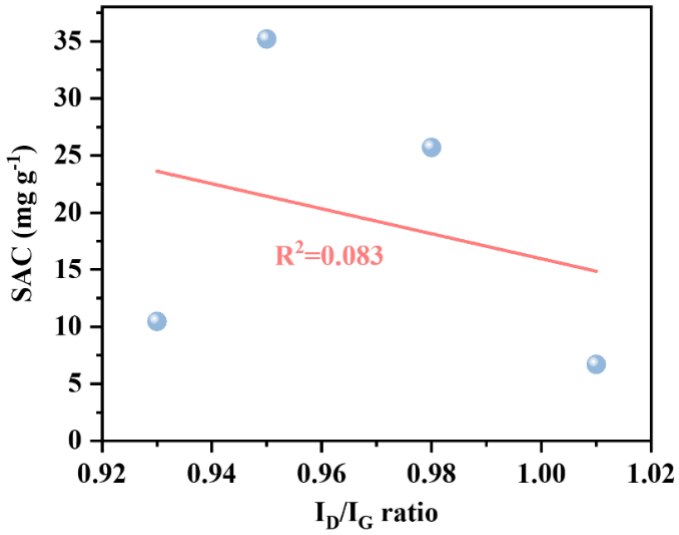

Figure S7. Correlation between I_D/I_G ration and the SAC.

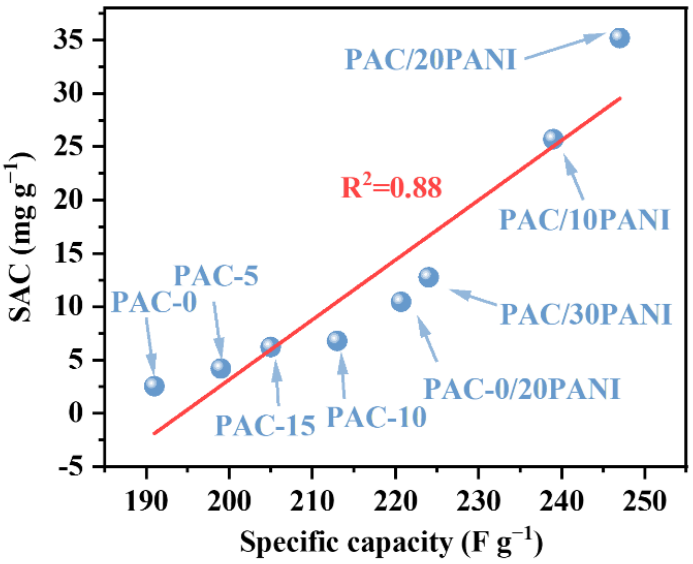

Figure S8. Correlation between specific capacity and the SAC.

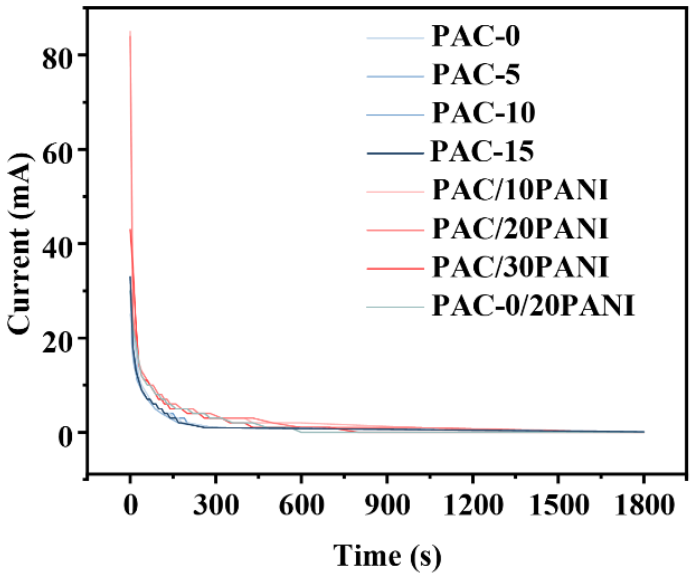

Figure S9. Current change of PACs and PAC/mPANI during deionization process.

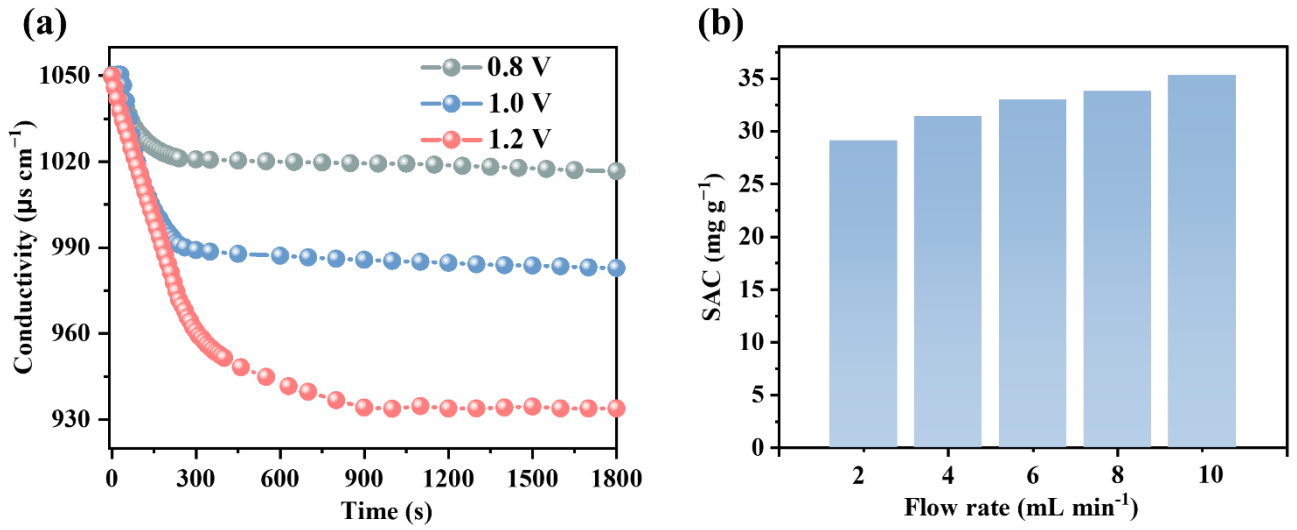

Figure S10. Conductivity variations of PAC/20PANI at different voltages (a); SAC of PAC/20PANI at different flow rates (b);

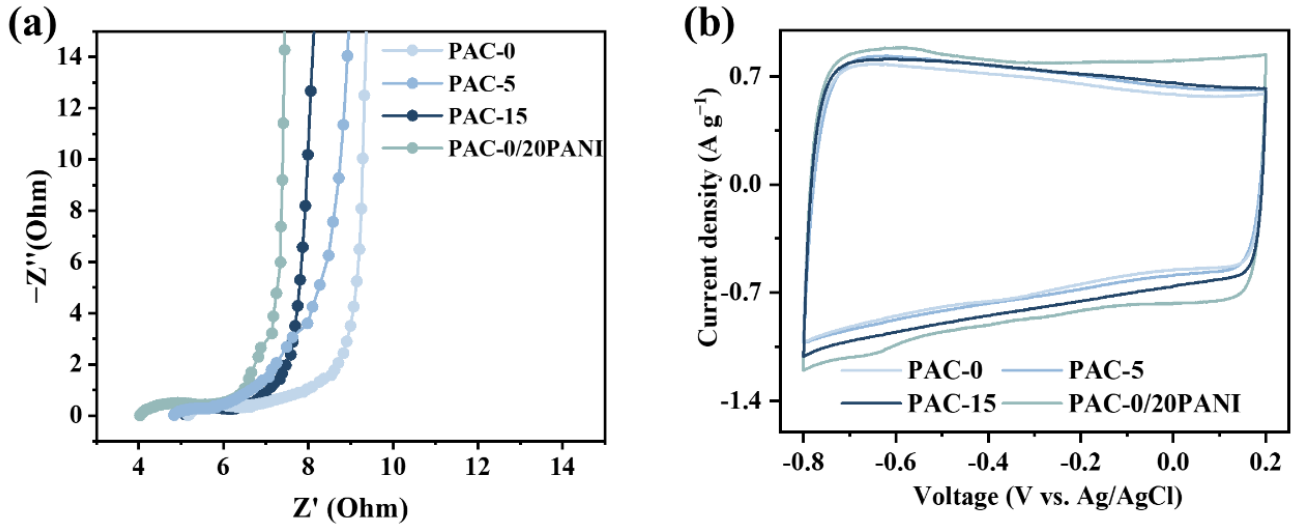

Figure S11. Electrochemical characterization of PAC-0, PAC-5, PAC-15 and PAC-0/20PANI in three-electrode system with 0.5 M NaCl solution as the electrolyte: EIS spectra in the frequency range of 0.01 Hz to 100 KHz of 10 mV amplitude (a); CV curves at scan rate of 5 mV s^{-1} (b).

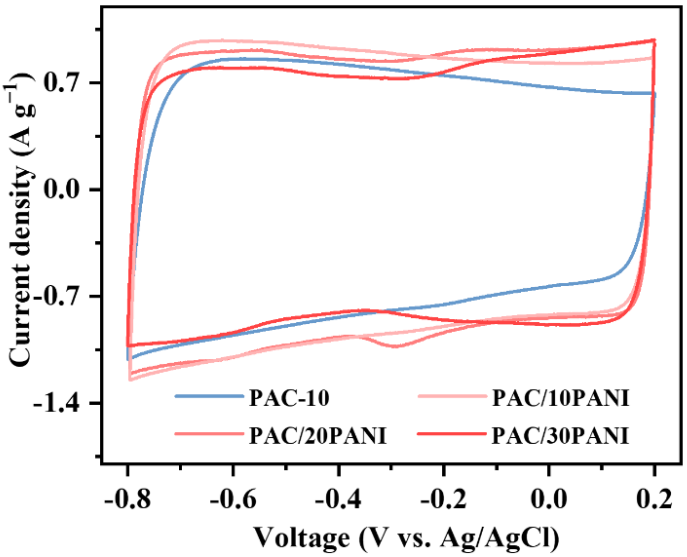

Figure S12. CV curves at scan rate of 5 mV $s^{-1}$of PAC-10, PAC/10PANI, PAC/20PANI and PAC/30PANI in three-electrode system with 0.5 M NaCl solution as the electrolyte.

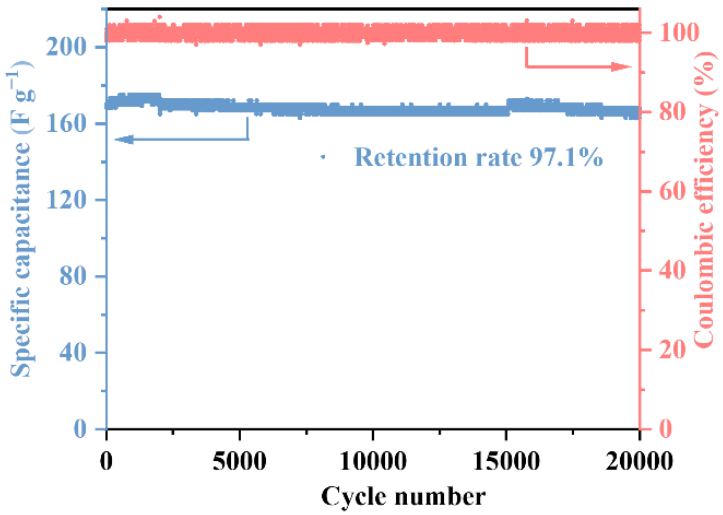

Figure S13. Electrochemical characterization of PAC/20PANI in button battery and with 1 M Na_2SO_4 as the electrolyte: Cycling performance at 1 A g^{-1} and voltage range is 0–1.2 V.

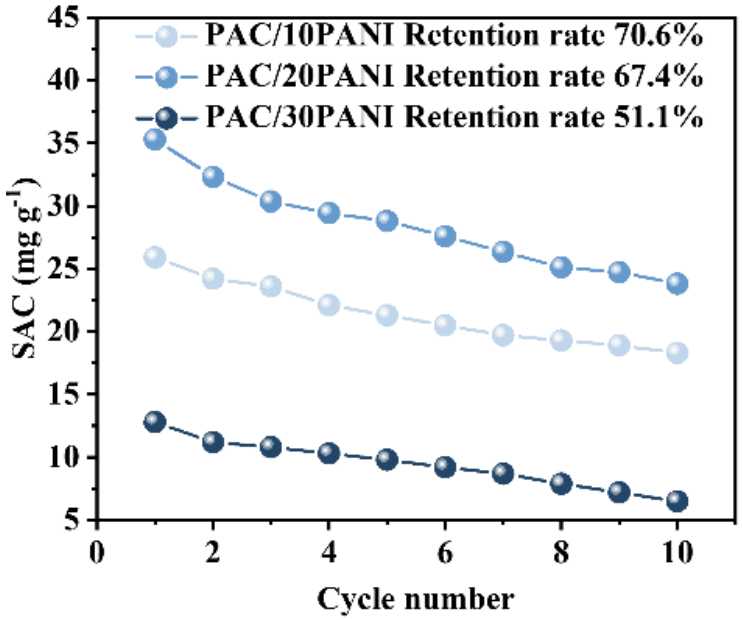

Figure S14. Electrode reversibility tests for PAC loaded with different amounts of PANI.

References

1 S. F. Evans, M. R. Ivancevic, D. J. Wilson, Z. D. Hood, S. P. Adhikari, A. K. Naskar, C. Tsouris and M. P. Paranthaman, *Desalination*, 2019, **464**, 25-32.

2 H. Wang, T. Yan, L. Shi, G. Chen, J. Zhang and D. Zhang, *ACS Appl. Mater.*, 2017, **5**, 3329-3338.

3 B. Pna, B. Jya, B. Gza and B. Jla, *Electrochim. Acta*, 2020, **339**, 135920.

4 S. Huo, W. Ni, Y. Zhao, X. Song, Y. Zhao, K. Li, H. Wang and M. Zhang, *J. Mater. Chem. A*, 2021, **9**, 3066-3076.

5 H. Wang, T. Yuan, L. Huang, Y. He, B. Wu, L. Hou, Q. Liao and W. Yang, *Sci. Total Environ.*, 2020, **720**, 137637.

6 Y. Zhu, G. Zhang, C. Xu and L. Wang, *ACS Appl. Mater.*, 2020, **12**, 29706-29716.

7 Y. Wu, G. Jiang, G. Liu, G. Lui, Z. P. Cano, Q. Li, Z. Zhang, A. Yu, Z. Zhang and Z. Chen, *J. Mater. Chem. A*, 2019, **7**, 15633-15639.